fractal and fractional

MDPI

Article

Mixed Convection of Fractional Nanofluids Considering Brownian Motion and Thermophoresis

Mingwen Chen [1], Yefan Tian [1], Weidong Yang [2] and Xuehui Chen [1,*]

[1] School of Mathematics and Physics, University of Science and Technology Beijing, Beijing 100083, China
[2] School of Energy and Environmental Engineering, University of Science and Technology Beijing, Beijing 100083, China
* Correspondence: xuehuichen@ustb.edu.cn

Abstract: In this paper, the mixed convective heat transfer mechanism of nanofluids is investigated. Based on the Buongiorno model, we develop a novel Cattaneo–Buongiorno model that reflects the non-local properties as well as Brownian motion and thermophoresis diffusion. Due to the highly non-linear character of the equations, the finite difference method is employed to numerically solve the governing equations. The effectiveness of the numerical method and the convergence order are presented. The results show that the rise in the fractional parameter δ enhances the energy transfer process of nanofluids, while the fractional parameter γ has the opposite effect. In addition, the effects of Brownian motion and thermophoresis diffusion parameters are also discussed. We infer that the flow and heat transfer mechanism of the viscoelastic nanofluids can be more clearly revealed by controlling the parameters in the Cattaneo–Buongiorno model.

Keywords: nanofluids; Brownian motion and thermophoresis; fractional derivative; mixed convection

check for updates

Citation: Chen, M.; Tian, Y.; Yang, W.; Chen, X. Mixed Convection of Fractional Nanofluids Considering Brownian Motion and Thermophoresis. *Fractal Fract.* **2022**, *6*, 584. https://doi.org/10.3390/fractalfract6100584

Academic Editor: Riccardo Caponetto

Received: 4 September 2022
Accepted: 8 October 2022
Published: 12 October 2022

1. Introduction

Compared with natural convection and forced convection, mixed convection is more common and significant in all areas of life, industry, and scientific research, and it holds great prospects for research, such as nuclear reactors, electronic cooling technology, and other industrial processes. More and more researchers are involved in the research of mixed convection. Fan et al. [1] analyzed the laminar mixed convective heat transfer in a level channel of nanofluids. Abu-Nada and Chamkha [2] numerically simulated a stable laminar mixed convective flow of a water–CuO nanofluid in a lid-driven cavity with wavy wall. Aaiza et al. [3] studied the energy transfer of the mixed convective unsteady magnetohydrodynamic (MHD) flow of nanofluids in saturated porous media channels. Aman et al. [4] analyzed the MHD mixed convection Poiseuille flow of gold nanoparticles, taking into account the effects of thermal radiation, chemical reaction, and thermal diffusion. Chakravarty et al. [5] employed the Darcy–Brinkman–Forchheimer model for numerical simulation to study the mixed convection heat transfer of fluids. Khanafer and Vafai [6] studied the double-diffusion mixed convective flow in a lid-driven vessel filled with a liquid-saturated porous medium. Moolya and Anbalgan [7] numerically investigated and optimized the influence of vital parameters on double-diffusion mixed convection. In addition, the stability of mixed convection under different specific conditions was also verified [8,9].

Recently, nanofluids have been widely used to improve various heat transfer properties based on their superior characteristics [10–12], such as macro and micro heat exchangers, aerospace applications, electronic equipment cooling, and other heat transfer enhancement fields. Choi first proposed the concept of the nanofluids [13]. Subsequently, Xuan et al. [14] refined the theory of thermal conductivity of nanofluids. In particular, for complex nanofluids, it is vital to introduce the improved constitution equation to describe the heat transfer phenomena. In 2006, the Buongiorno model was proposed [15], which concluded that

Brownian motion and thermophoresis are the significant slip mechanisms for nanofluids, and explained the principles of the Brownian and thermophoresis diffusion. Since then, the model has been broadly applied by researchers, and the research on the nanofluids made great progress. Ahmed et al. [16] used the Buongiorno model to study the flow of nanofluids in a heat-generated porous medium-filled wavy enclosures. Bansch et al. [17] applied the Buongiorno model to analyze the existence of steady-state problem solutions of convection transfer of nanofluids. Sohail et al. [18] numerically calculated the flow of fluid on a stretched sheet applying the Buongiorno model. However, the heat and mass diffusion in the model adopts the classical Fourier and Fick's laws, ignoring thermal relaxation and mass relaxation effects. In subsequent studies, scholars made different improvements to the model. Rana et al. [19] employed the modified Buongiorno model to study 3D flow and heat transfer of nanoliquids. Puneeth et al. [20] applied the modified Buongiorno model to study the jet flow of ternary nanofluids. It is worth noting that traditional constitutive relations cannot be used to describe the special properties of nanofluids, and fractional calculus theory is widely applied because of its non-locality and long memory characteristics [21,22]. Aman et al. [23] researched the heat and mass transfer of graphene nanofluids through a vertical plate by fractional derivative. Zhao et al. [24] first introduced fractional order into boundary layer equations to study the heat transfer of unstable natural convection boundary layers. Chen et al. [25] discussed the boundary layer flow of fractional viscoelastic MHD fluids on a stretched thin plate. Liu et al. [26] introduced fractional derivatives to describe heat conduction in the Cattaneo–Christov model. Cao et al. [27] applied the fractional Maxwell model to analyze the flow and heat of nanofluids on a moving plate. Zhao et al. [28] described the unsteady Marangoni convection of fractional Maxwell fluids. Recently, the double fractional Maxwell model was widely studied by researchers [29–32]. The results display that the double fractional Maxwell model is more flexible and accurate in explaining the flow of viscoelastic fluids.

In recent years, researchers applied fractional calculus theory to the Buongiorno model and made different improvements and revisions. Shen et al. [33] introduced the Cattaneo thermal conductivity model with time fractional derivative in the Buongiorno model to describe the abnormal heat transfer of nanofluids. After that, Zhang et al. [34] introduced the spatial fractional derivative based on the improved Buongiorno model to characterize the non-local behavior of nanofluids. To the best of our knowledge, the fractional constitutive model is more effective and reliable to describe the flow and heat transfer phenomena of the viscoelastic nanofluids. The Cattaneo thermal conductivity model with double time fractional derivatives is introduced to modify the Buongiorno model.

Based on the above discussions, in this paper, a generalized Cattaneo–Buongiorno constitutive model is proposed to explore the heat and mass transfer of nanofluids in mixed convection. The governing equations are resolved by the finite difference method. The accuracy of the numerical algorithm is verified. In addition, the effects of diverse important parameters on heat transfer and mass transfer are depicted graphically and analyzed.

2. Mathematical Formulation

We propose a generalized Cattaneo–Buongiorno constitutive model, defined as follows:

$$\boldsymbol{q} + \lambda_2^{\delta} \frac{\partial^{\delta} \boldsymbol{q}}{\partial t^{\delta}} = -K \lambda_2^{\gamma} \frac{\partial^{\gamma-1}}{\partial t^{\gamma-1}} \left(\frac{\partial T}{\partial y} \right) + h_p \cdot \boldsymbol{j}_p, 0 \le \delta \le \gamma \le 1 \quad (1)$$

where $\boldsymbol{q}$ is the heat flux, $\lambda_2 = k/K$ is the temperature relaxation time, k is the thermal conductivity, δ and γ are the fractional parameters, and $\partial^{\delta}/\partial t^{\delta}$ and $\partial^{\gamma-1}/\partial t^{\gamma-1}$ are the Caputo's fractional derivatives. Subscripts nf and p represent nanofluids and nanosolids, respectively, $h_p = c_p T$ is the specific enthalpy, and $\boldsymbol{j_p}$ is the diffusion mass flux, which is expressed as [27]:

$$\boldsymbol{j_p} = \boldsymbol{j_{p,B}} + \boldsymbol{j_{p,T}} = -\rho_p D_B \nabla C - \rho_p D_T \frac{\nabla T}{T_0}, \quad (2)$$

where ρ_p is the mass density, and D_B and D_T express the Brownian diffusion coefficient and thermophoresis diffusion coefficient, respectively. T is the nanofluids temperature. The fractional Maxwell model is introduced as the constitution relationship of the viscoelastic nanofluids [29].

Consider mixed convection of fractional Maxwell nanofluids between two infinitely long parallel plates, which is caused by the temperature difference. The distance between the two parallel plates is d, and the system of rectangular coordinates (x, y) is selected. The x-axis is parallel to the flow direction of the fluid, and the y-axis is perpendicular to the flow direction of the fluid. A geometry image of the system is shown in Figure 1. The equations of the velocity, temperature, and concentration fields can be expressed as:

$$\rho_{nf}\frac{\partial u}{\partial t} = -\nabla p + \nabla \cdot \boldsymbol{\tau} + \rho_{nf} g, \tag{3}$$

$$(\rho c_p)_{nf}\frac{\partial T}{\partial t} = -\nabla \cdot \boldsymbol{q} + h_p \nabla \cdot \boldsymbol{j}_p, \tag{4}$$

$$\frac{\partial C}{\partial t} = -\frac{1}{\rho_p}\nabla \cdot \boldsymbol{j}_p - k_r(C - C_0), \tag{5}$$

with the boundary and initial conditions:

$$t = 0 : u = 0, T = T_0, C = C_0; y = 0 : u = 0, T = T_0, C = C_0; y = d : u = 0, T = T_w, C = C_w, \tag{6}$$

where ρ_{nf} is the density of nanofluids and ∇p is the pressure gradient, expressed as $\nabla p = \partial p/\partial x = -\rho_\infty g$. By invoking Boussinesq approximation, we have $\rho_\infty - \rho_{nf} = \rho_{nf}\beta_{nf}(T - T_0)$. $(\rho\beta)_{nf}$ is the thermal expansion coefficient, g is the gravitational acceleration, $(\rho c_p)_{nf}$ is the capacitance, and k_r is the chemical reaction parameter.

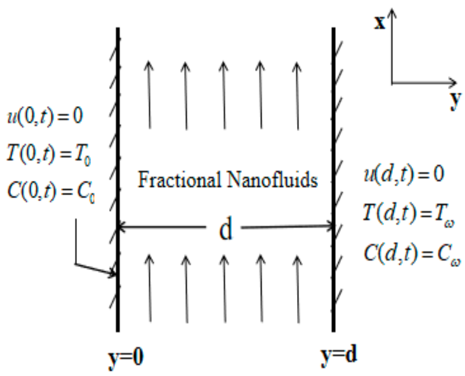

Figure 1. Geometric sketch.

The fractional Maxwell model of nanofluids [29] is substituted into the momentum Equation (3). The generalized Cattaneo–Buongiorno constitutive Equation (1) is substituted into energy Equation (4) and concentration Equation (5). The governing equations of nanofluids mixed convection model can be expressed as follows:

$$\left(\lambda_1^{1-\beta}\frac{\partial^{1-\beta}}{\partial t^{1-\beta}} + \lambda_1^{1+\alpha-\beta}\frac{\partial^{1+\alpha-\beta}}{\partial t^{1+\alpha-\beta}}\right)\left(\frac{\partial u}{\partial t} - (\beta_T)_{nf} g(T - T_0)\right) = v\frac{\partial^2 u}{\partial y^2}, \tag{7}$$

$$\left(\lambda_2^{1-\gamma}\frac{\partial^{1-\gamma}}{\partial t^{1-\gamma}} + \lambda_2^{1+\delta-\gamma}\frac{\partial^{1+\delta-\gamma}}{\partial t^{1+\delta-\gamma}}\right)\frac{\partial T}{\partial t} = \frac{k}{(\rho c_p)_{nf}}\frac{\partial^2 T}{\partial y^2} + \sigma\lambda_2^{1-\gamma}\frac{\partial^{1-\gamma}}{\partial t^{1-\gamma}}\left(D_B\frac{\partial C}{\partial y}\frac{\partial T}{\partial y} + \frac{D_T}{T_0}\left(\frac{\partial T}{\partial y}\right)^2\right) - \sigma\lambda_2^{1+\delta-\gamma}\frac{\partial^{1+\delta-\gamma}}{\partial t^{1+\delta-\gamma}}\left(D_B T\frac{\partial^2 C}{\partial y^2} + \frac{D_T T}{T_0}\frac{\partial^2 T}{\partial y^2}\right), \tag{8}$$

$$\frac{\partial C}{\partial t} = D_B\frac{\partial^2 C}{\partial y^2} + \frac{D_T}{T_0}\frac{\partial^2 T}{\partial y^2} - k_r(C - C_0), \tag{9}$$

where α and β are the fractional parameters of shear stress and shear strain, respectively. $\sigma = (\rho c)_p$ is the heat capacity and $v = \mu/\rho$ is the kinematic viscosity of nanofluids.

By introducing the following dimensionless variables:

$$u^* = \frac{u}{U_0}, x^* = \frac{x}{d}, y^* = \frac{y}{d}, t^* = \frac{tU_0}{d}, {\lambda_1}^* = \frac{\lambda_1 U_0}{d},$$

$$\lambda_2^* = \frac{\lambda_2 U_0}{d}, T^* = \frac{T - T_0}{T_w - T_0}, C^* = \frac{C - C_0}{C_w - C_0}, {k_r}^* = \frac{k_r d}{U_0},$$

the dimensionless governing equations can be written as (ignoring symbols $*$ for calculation convenience):

$$\left(\lambda_1^{1-\beta}\frac{\partial^{1-\beta}}{\partial t^{1-\beta}} + \lambda_1^{1+\alpha-\beta}\frac{\partial^{1+\alpha-\beta}}{\partial t^{1+\alpha-\beta}}\right)\left(\mathrm{Re}\frac{\partial u}{\partial t} - GrT\right) = \frac{\partial^2 u}{\partial y^2}, \tag{10}$$

$$\left(\lambda_2^{1-\gamma}\frac{\partial^{1-\gamma}}{\partial t^{1-\gamma}} + \lambda_2^{1+\delta-\gamma}\frac{\partial^{1+\delta-\gamma}}{\partial t^{1+\delta-\gamma}}\right)\frac{\partial T}{\partial t} = \frac{1}{\mathrm{Re}\cdot\mathrm{Pr}}\frac{\partial^2 T}{\partial y^2} + \lambda_2^{1-\gamma}\frac{\partial^{1-\gamma}}{\partial t^{1-\gamma}}\left(\frac{Nb}{\mathrm{Re}}\frac{\partial C}{\partial y}\frac{\partial T}{\partial y} + \frac{Nt}{\mathrm{Re}}\left(\frac{\partial T}{\partial y}\right)^2\right) - \lambda_2^{1+\delta-\gamma}\frac{\partial^{1+\delta-\gamma}}{\partial t^{1+\delta-\gamma}}\left(\frac{Nb}{\mathrm{Re}}T\frac{\partial^2 C}{\partial y^2} + \frac{Nt}{\mathrm{Re}}T\frac{\partial^2 T}{\partial y^2}\right), \tag{11}$$

$$\frac{\partial C}{\partial t} = \frac{1}{\mathrm{Re}\cdot Ln}\frac{\partial^2 C}{\partial y^2} + \frac{1}{\mathrm{Re}\cdot Ln}\frac{Nt}{Nb}\frac{\partial^2 T}{\partial y^2} - k_r C, \tag{12}$$

where Re is the Reynolds number, Gr is the thermal Grashof number, α_m is the thermal diffusion coefficient of nanofluids, Pr is the generalized Prandtl number, Nt is the thermophoresis parameter, Nb is the Brownian motion parameter, and Ln is the Lewis number. Their expressions are as follows:

$$\mathrm{Re} = \frac{\rho U_0 d}{\mu}, Gr = \frac{g(\beta_T)_{nf}(T_w - T_0)d^2}{U_0 v}, \alpha_m = \frac{k}{(\rho c_p)_{nf}}, \mathrm{Pr} = \frac{v}{\alpha_m}, Nt = \frac{\sigma D_T(T_w - T_0)}{T_0 v}, Nb = \frac{\sigma D_B(C_w - C_0)}{v}, Ln = \frac{v}{D_B}.$$

The initial and boundary conditions are:

$$t = 0 : u = 0, T = 0, C = 0; y = 0 : u = 0, T = 0, C = 0; y = 1 : u = 0, T = 1, C = 1. \tag{13}$$

3. Numerical Technique

The finite difference method is applied to solve the dimensionless Equations (10)–(12). Denote $x_i = i\Delta x(i = 0, 1, 2, \cdots, M), y_j = j\Delta y(j = 0, 1, 2, \cdots, N), t_k = k\Delta t(k = 0, 1, 2, \cdots, L)$, where $\Delta x = X_{\max}/M$ and $\Delta y = Y_{\max}/N$ are the space steps, and Δt is the time step. The time fractional derivative is worked out by employing the L1 algorithm.

First, the L1 algorithm is imported as $(0 < \alpha < 1)$ [35]:

$$\begin{aligned}\frac{\partial^\alpha f(t_k)}{\partial t^\alpha} &= \frac{\Delta t^{-\alpha}}{\Gamma(2-\alpha)}\sum_{s=0}^{k-1}\alpha_s[f(t_{k-s}) - f(t_{k-s-1})] + \mathrm{O}(\Delta t^{2-\alpha}) \\ &= \frac{\Delta t^{-\alpha}}{\Gamma(2-\alpha)}\left[f(t_k) - \alpha_{k-1}f(t_0) - \sum_{s=1}^{k-1}(\alpha_{s-1} - \alpha_s)f(t_{k-s})\right] + \mathrm{O}(\Delta t^{2-\alpha}),\end{aligned} \tag{14}$$

where $\alpha_s = (s+1)^{1-\alpha} - s^{1-\alpha}, s = 0, 1, 2, \ldots, R$

Second, the integer order discretization in the system of control equations is as follows:

$$\left.\frac{\partial u}{\partial t}\right|_{t=t_k} = \frac{u_{i,j}^k - u_{i,j}^{k-1}}{\Delta t} + \mathrm{O}(\Delta t), \tag{15}$$

$$\left.\frac{\partial^2 u}{\partial y^2}\right|_{t=t_k} = \frac{u_{i,j+1}^k - 2u_{i,j}^k + u_{i,j-1}^k}{\Delta y^2} + \mathrm{O}(\Delta y^2), \tag{16}$$

$$\left.\frac{\partial C}{\partial y}\frac{\partial T}{\partial y}\right|_{t=t_k} = \frac{C_{i,j}^{k-1} - C_{i,j-1}^{k-1}}{\Delta y}\frac{T_{i,j}^k - T_{i,j-1}^k}{\Delta y} + \mathrm{O}(\Delta t + \Delta y), \tag{17}$$

$$\left.\left(\frac{\partial T}{\partial y}\right)^2\right|_{t=t_k} = \frac{T_{i,j}^{k-1} - T_{i.j-1}^{k-1}}{\Delta y}\frac{T_{i,j}^k - T_{i,j-1}^k}{\Delta y} + \mathrm{O}(\Delta t + \Delta y), \tag{18}$$

$$T\frac{\partial^2 C}{\partial y^2}\bigg|_{t=t_k} = T_{i,j}^{k}\frac{C_{i,j+1}^{k-1}-2C_{i,j}^{k-1}+C_{i,j-1}^{k-1}}{\Delta y^2}+\mathrm{O}(\Delta t+\Delta y^2), \tag{19}$$

$$T\frac{\partial^2 T}{\partial y^2}\bigg|_{t=t_k} = T_{i,j}^{k-1}\frac{T_{i,j+1}^{k}-2T_{i,j}^{k}+T_{i,j-1}^{k}}{\Delta y^2}+\mathrm{O}(\Delta t+\Delta y^2). \tag{20}$$

Third, we disperse time fractional derivatives at $\left(x_i, y_j, t_k\right)$ $(0<\alpha<1)$ as follows:

$$\frac{\partial^\alpha}{\partial t^\alpha}\left(\frac{\partial u}{\partial t}\right)\bigg|_{t=t_k} = \frac{\Delta t^{-1-\alpha}}{\Gamma(2-\alpha)}\left(u_{i,j}^{k}-u_{i,j}^{k-1}-\sum_{s=1}^{k-1}(\alpha_{s-1}-\alpha_s)\left(u_{i,j}^{k-s}-u_{i,j}^{k-s-1}\right)\right)+\mathrm{O}(\Delta t), \tag{21}$$

$$\frac{\partial^\alpha T}{\partial t^\alpha}\bigg|_{t=t_k} = \frac{\Delta t^{-\alpha}}{\Gamma(2-\alpha)}\left(T_{i,j}^{k}-\sum_{s=1}^{k-1}(\alpha_{s-1}-\alpha_s)T_{i,j}^{k-s}\right)+\mathrm{O}\left(\Delta t^{2-\alpha}\right), \tag{22}$$

$$\frac{\partial^\alpha}{\partial t^\alpha}\left(\frac{\partial C}{\partial y}\frac{\partial T}{\partial y}\right)\bigg|_{t=t_k} = \frac{\Delta t^{-\alpha}}{\Gamma(2-\alpha)\Delta y^2}\left(\left(C_{i,j}^{k-1}-C_{i,j-1}^{k-1}\right)\left(T_{i,j}^{k}-T_{i,j-1}^{k}\right)-\sum_{s=1}^{k-1}(\alpha_{s-1}-\alpha_s)\left(C_{i,j}^{k-s-1}-C_{i,j-1}^{k-s-1}\right)\left(T_{i,j}^{k-s}-T_{i,j-1}^{k-s}\right)\right)+\mathrm{O}(\Delta t+\Delta y), \tag{23}$$

$$\frac{\partial^\alpha}{\partial t^\alpha}\left(T\frac{\partial^2 C}{\partial y^2}\right)\bigg|_{t=t_k} = \frac{\Delta t^{-\alpha}}{\Gamma(2-\alpha)\Delta y^2}\left(T_{i,j}^{k}\left(C_{i,j+1}^{k-1}-2C_{i,j}^{k-1}+C_{i,j-1}^{k-1}\right)-\sum_{s=1}^{k-1}(\alpha_{s-1}-\alpha_s)T_{i,j}^{k-s}\left(C_{i,j+1}^{k-s-1}-2C_{i,j}^{k-s-1}+C_{i,j-1}^{k-s-1}\right)\right)+\mathrm{O}(\Delta t+\Delta y^2). \tag{24}$$

Then, the results of the iterative Equations of (10)–(12) are:

$$-r_8u_{i,j-1}^{k}+(r_6+r_7+2r_8)u_{i,j}^{k}-r_8u_{i,j+1}^{k}=(r_6+r_7)u_{i,j}^{k-1}+r_6A_1+r_7A_2+r_6r_{10}\left(T_{i,j}^{k}-A_3\right)+r_7r_{10}\left(T_{i,j}^{k}-A_4\right)+R_{1i,j}^{k}, \tag{25}$$

$$\begin{aligned}&\left(-r_3+r_1r_4\left(C_{i,j}^{k-1}-C_{i,j-1}^{k-1}\right)+r_1r_5\left(T_{i,j}^{k-1}-T_{i,j-1}^{k-1}\right)+r_2r_5T_{i,j}^{k-1}\right)T_{i,j-1}^{k}+\left(-r_3+r_2r_5T_{i,j}^{k-1}\right)T_{i,j+1}^{k}\\&+\left(r_1+r_2+2r_3-r_1r_4\left(C_{i,j}^{k-1}-C_{i,j-1}^{k-1}\right)-r_1r_5\left(T_{i,j}^{k-1}-T_{i,j-1}^{k-1}\right)+r_2r_4\left(C_{i,j+1}^{k-1}-2C_{i,j}^{k-1}+C_{i,j-1}^{k-1}\right)-2r_2r_5T_{i,j}^{k-1}\right)T_{i,j}^{k}\\&=(r_1+r_2)T_{i,j}^{k-1}+r_1B_1+r_2B_2-r_1r_4B_3-r_1r_5B_4+r_2r_4B_5+r_2r_5B_6+R_{2i,j}^{k},\end{aligned} \tag{26}$$

$$-r_9C_{i,j-1}^{k}+(1+2r_9+k_r\Delta t)C_{i,j}^{k}-r_9C_{i,j+1}^{k}=C_{i,j}^{k-1}+r_9\frac{Nt}{Nb}\left(T_{i,j+1}^{k}-2T_{i,j}^{k}+T_{i,j-1}^{k}\right)+R_{3i,j}^{k}. \tag{27}$$

where $|R_1|\le C(\Delta t+\Delta y^2)$, $|R_2|\le C(\Delta t+\Delta y)$, $|R_3|\le C(\Delta t+\Delta y^2)$ and

$$r_1=\frac{\lambda_2^{1-\gamma}\Delta t^{-(1-\gamma)}}{\Gamma(2-(1-\gamma))}, r_2=\frac{\lambda_2^{1+\delta-\gamma}\Delta t^{-(1+\delta-\gamma)}}{\Gamma(2-(1+\delta-\gamma))}, r_3=\frac{\Delta t}{\mathrm{Re}\cdot\mathrm{Pr}\Delta y^2},$$

$$r_4=\frac{Nb}{\mathrm{Re}}\frac{\Delta t}{\Delta y^2}, r_5=\frac{Nt}{\mathrm{Re}}\frac{\Delta t}{\Delta y^2}, r_6=\frac{\lambda_1^{1-\beta}\Delta t^{-(1-\beta)}}{\Gamma(2-(1-\beta))}, r_7=\frac{\lambda_1^{1+\alpha-\beta}\Delta t^{-(1+\alpha-\beta)}}{\Gamma(2-(1+\alpha-\beta))},$$

$$r_8=\frac{\Delta t}{\mathrm{Re}\cdot\Delta y^2}, r_9=\frac{\Delta t}{\mathrm{Re}\cdot Ln\Delta y^2}, r_{10}=\frac{Gr\Delta t}{\mathrm{Re}},$$

$$A_1=\sum_{s=1}^{k-1}[(1-\beta)_{s-1}-(1-\beta)_s]\left(u_{i,j}^{k-s}-u_{i,j}^{k-s-1}\right),$$

$$A_2=\sum_{s=1}^{k-1}[(1+\alpha-\beta)_{s-1}-(1+\alpha-\beta)_s]\left(u_{i,j}^{k-s}-u_{i,j}^{k-s-1}\right),$$

$$A_3=\sum_{s=1}^{k-1}[(1-\beta)_{s-1}-(1-\beta)_s]T_{i,j}^{k-s},$$

$$A_4=\sum_{s=1}^{k-1}[(1+\alpha-\beta)_{s-1}-(1+\alpha-\beta)_s]T_{i,j}^{k-s},$$

$$B_1=\sum_{s=1}^{k-1}[(1-\gamma)_{s-1}-(1-\gamma)_s](T_{i,j}^{k-s}-T_{i,j}^{k-s-1}),$$

$$B_2=\sum_{s=1}^{k-1}[(1+\delta-\gamma)_{s-1}-(1+\delta-\gamma)_s](T_{i,j}^{k-s}-T_{i,j}^{k-s-1}),$$

$$B_3 = \sum_{s=1}^{k-1}[(1-\gamma)_{s-1} - (1-\gamma)_s]\left(C_{i,j}^{k-s-1} - C_{i,j-1}^{k-s-1}\right)(T_{i,j}^{k-s} - T_{i,j-1}^{k-s}),$$

$$B_4 = \sum_{s=1}^{k-1}[(1-\gamma)_{s-1} - (1-\gamma)_s]\left(T_{i,j}^{k-s-1} - T_{i,j-1}^{k-s-1}\right)(T_{i,j}^{k-s} - T_{i,j-1}^{k-s}),$$

$$B_5 = \sum_{s=1}^{k-1}[(1+\delta-\gamma)_{s-1} - (1+\delta-\gamma)_s]T_{i,j}^{k-s}\left(C_{i,j+1}^{k-s-1} - 2C_{i,j}^{k-s-1} + C_{i,j-1}^{k-s-1}\right),$$

$$B_6 = \sum_{s=1}^{k-1}[(1+\delta-\gamma)_{s-1} - (1+\delta-\gamma)_s]T_{i,j}^{k-s-1}\left(T_{i,j+1}^{k-s} - 2T_{i,j}^{k-s} + T_{i,j-1}^{k-s}\right).$$

The initial and boundary conditions of the discrete scheme are:

$$t = 0 : u = 0, T = 0, C = 0; y = 0 : u = 0, T = 0, C = 0; y = N : u = 0, T = 1, C = 1. \tag{28}$$

4. Validation of the Numerical Method

To examine the validity of the numerical method, the source terms $f_1(x,y,t)$, $f_2(x,y,t)$, and $f_3(x,y,t)$ are introduced into the governing equations. The expressions of the source terms are obtained in the governing equations through the analytical solutions. Next, a set of numerical solutions are acquired by the numerical method for comparison with the analytical solutions. As follows:

$$\left(\lambda_1^{1-\beta}\frac{\partial^{1-\beta}}{\partial t^{1-\beta}} + \lambda_1^{1+\alpha-\beta}\frac{\partial^{1+\alpha-\beta}}{\partial t^{1+\alpha-\beta}}\right)\left(\mathrm{Re}\frac{\partial u}{\partial t} - GrT\right) = \frac{\partial^2 u}{\partial y^2} + f_1(y,t), \tag{29}$$

$$\begin{aligned}\left(\lambda_2^{1-\gamma}\frac{\partial^{1-\gamma}}{\partial t^{1-\gamma}} + \lambda_2^{1+\delta-\gamma}\frac{\partial^{1+\delta-\gamma}}{\partial t^{1+\delta-\gamma}}\right)\frac{\partial T}{\partial t} = \frac{1}{\mathrm{Re}\cdot\mathrm{Pr}}\frac{\partial^2 T}{\partial y^2} + \lambda_2^{1-\gamma}\frac{\partial^{1-\gamma}}{\partial t^{1-\gamma}}\left(\frac{Nb}{\mathrm{Re}}\frac{\partial C}{\partial y}\frac{\partial T}{\partial y} + \frac{Nt}{\mathrm{Re}}\left(\frac{\partial T}{\partial y}\right)^2\right)\\ -\lambda_2^{1+\delta-\gamma}\frac{\partial^{1+\delta-\gamma}}{\partial t^{1+\delta-\gamma}}\left(\frac{Nb}{\mathrm{Re}}T\frac{\partial^2 C}{\partial y^2} + \frac{Nt}{\mathrm{Re}}T\frac{\partial^2 T}{\partial y^2}\right) + f_2(y,t),\end{aligned} \tag{30}$$

$$\frac{\partial C}{\partial t} = \frac{1}{\mathrm{Re}\cdot Ln}\frac{\partial^2 C}{\partial y^2} + \frac{1}{\mathrm{Re}\cdot Ln}\frac{Nt}{Nb}\frac{\partial^2 T}{\partial y^2} - k_r C + f_3(y,t), \tag{31}$$

with the new initial and boundary conditions:

$$t = 0 : u = 0, T = 0, C = 0; y = 0 : u = 0, T = 0, C = 0; y = 1 : u = 0, T = 0, C = 0. \tag{32}$$

where

$$\begin{aligned} f_1(y,t) = &-\frac{2\lambda_1^{1-\beta}y^2(y-1)^2\left(t^{1+\beta}Gr\Gamma(1+\beta) - t^{\beta}\mathrm{Re}\Gamma(2+\beta)\right)}{\Gamma(1+\beta)\Gamma(2+\beta)}\\ &-\frac{2\lambda_1^{1+\alpha-\beta}y^2(y-1)^2(t^{1-\alpha+\beta}Gr\Gamma(1-\alpha+\beta) - t^{-\alpha+\beta}\mathrm{Re}\Gamma(2-\alpha+\beta))}{\Gamma(1-\alpha+\beta)\Gamma(2-\alpha+\beta)}\\ &-2(1-y)^2t^2 + 8y(1-y)t^2 - 2y^2t^2,\end{aligned} \tag{33}$$

$$\begin{aligned} f_2(y,t) = &\frac{2\lambda_2^{1-\gamma}t^{\gamma}y^2(y-1)^2}{\Gamma(1+\gamma)} + \frac{2\lambda_2^{1+\delta-\gamma}t^{-\delta+\gamma}y^2(y-1)^2}{\Gamma(1-\delta+\gamma)} - \frac{2(1-y)^2t^2 - 8y(1-y)t^2 + 2y^2t^2}{\mathrm{Re}\cdot\mathrm{Pr}}\\ &-\frac{96\lambda_2^{1-\gamma}t^{3+\gamma}y^2(2y^2-3y+1)^2(Nb+Nt)}{\mathrm{Re}\cdot\Gamma(4+\gamma)}\\ &+\frac{48\lambda_2^{1+\delta-\gamma}t^{3-\delta+\gamma}y^2(y-1)^2(6y^2Nb+6y^2Nt-6yNb-6yNt+Nb+Nt)}{\mathrm{Re}\cdot\Gamma(4-\delta+\gamma)},\end{aligned} \tag{34}$$

$$f_3(y,t) = 2y^2(1-y)^2t - \frac{(2-12y+12y^2)t^2(1+Nt/Nb)}{\mathrm{Re}\cdot Ln} + Kr\cdot y^2(1-y)^2t^2. \tag{35}$$

The following analytical solutions are obtained:

$$u(y,t) = T(y,t) = C(y,t) = y^2(1-y)^2t^2. \tag{36}$$

In Figure 2, the velocity, temperature, and concentration distributions of nanofluids along t direction are given by numerical and analytical solutions, respectively. It can be seen that the arithmetic solutions coincide well with the analytical solutions, which shows the correctness of the numerical algorithm. To examine the convergence order of the numerical method, Tables 1–3 give the L_2 error, the L_∞ error, and the convergence order of the momentum, energy, and concentration equations for different time steps Δt. The convergence order can reach the first order, as we expected.

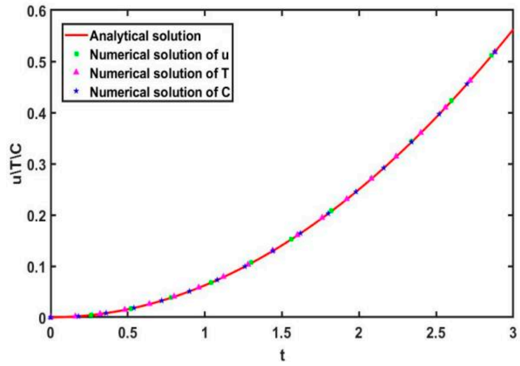

Figure 2. Comparisons between the analytical solutions and numerical solutions of t.

Table 1. The truncation error and convergence order of velocity u with $\Delta y = 0.01$.

Δt	L_2 Error	Order	L_∞ Error	Order
0.1	3.0723×10^{-3}	-	4.4143×10^{-3}	-
0.05	1.5496×10^{-3}	0.9874	2.2262×10^{-3}	0.9876
0.025	7.7837×10^{-4}	0.9934	1.1181×10^{-3}	0.9935
0.0125	3.9022×10^{-4}	0.9962	5.6051×10^{-4}	0.9962

Table 2. The truncation error and convergence order of temperature T with $\Delta y = 0.01$.

Δt	L_2 Error	Order	L_∞ Error	Order
0.1	1.8800×10^{-3}	-	2.7568×10^{-3}	-
0.05	9.6757×10^{-4}	0.9583	1.4177×10^{-3}	0.9594
0.025	4.9147×10^{-4}	0.9773	7.1997×10^{-4}	0.9775
0.0125	2.4796×10^{-4}	0.9870	3.6353×10^{-4}	0.9859

Table 3. The truncation error and convergence order of concentration C with $\Delta y = 0.01$.

Δt	L_2 Error	Order	L_∞ Error	Order
0.1	4.0470×10^{-4}	-	5.4928×10^{-4}	-
0.05	1.8991×10^{-4}	1.0915	2.5773×10^{-4}	1.0917
0.025	9.1774×10^{-5}	1.0492	1.2564×10^{-4}	1.0366
0.0125	4.5249×10^{-5}	1.0202	6.3692×10^{-5}	0.9801

5. Results and Discussion

The governing Equations (10)–(12) with conditions (13) are resolved by the finite difference method. The space and time steps are $\Delta y = 0.01, \Delta t = 0.02$, respectively. In this section, we mainly discuss the influence of fractional parameters, Brownian parameters, and thermophoresis parameters on the temperature and concentration of the nanofluids.

5.1. Effects of the Fractional Parameters on the Temperature Field

Figure 3 describes the relationship between fractional parameters δ and γ and the temperature of nanofluids in the y direction. Particularly, the temperature distributions under different fractional order parameter δ when $\gamma = 0.9$ are shown in Figure 3a. With the increase in δ in the same location, the temperature profile rises uniformly, which means that the heat transfer process of the nanofluids is enhanced with the augment in the fractional parameter δ. Figure 3b gives the temperature distributions under different fractional order parameter γ when $\delta = 0.1$. The results manifest that the greater the fractional parameter γ, the lower the temperature of the nanofluids. It follows that the nanofluids heat transfer process is weakened with the growth of fractional parameter γ.

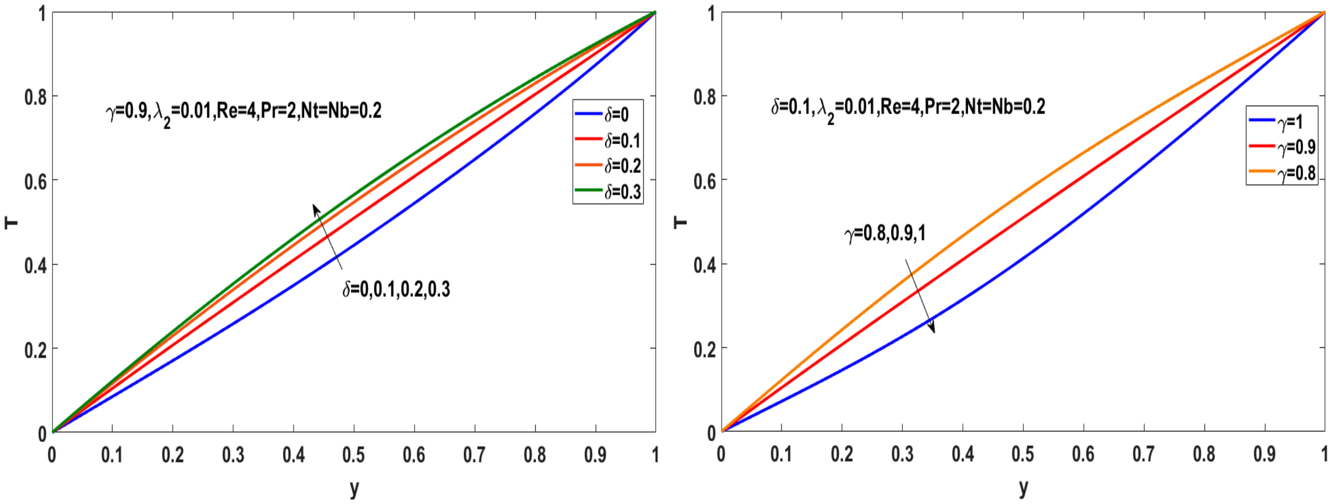

(**a**) (**b**)

Figure 3. Temperature distributions with respect to y: (**a**) for different δ; (**b**) for different γ.

Figure 4 shows the effect of different fractional order parameters δ and γ on the temperature of nanofluids in the t direction. Figure 4a reveals that with the passage of time, the temperature always first elevates to a peak, then decreases, and finally reaches a stable value. Figure 4b describes the temperature distributions when $\gamma = 1, 0.9, 0.8, 0.7$. There is a peak in temperature as the fractional parameter γ decreases. A smaller γ corresponds to a higher temperature peak. Similarly, for each value of γ, the temperature eventually reaches a stable level and does not change any more.

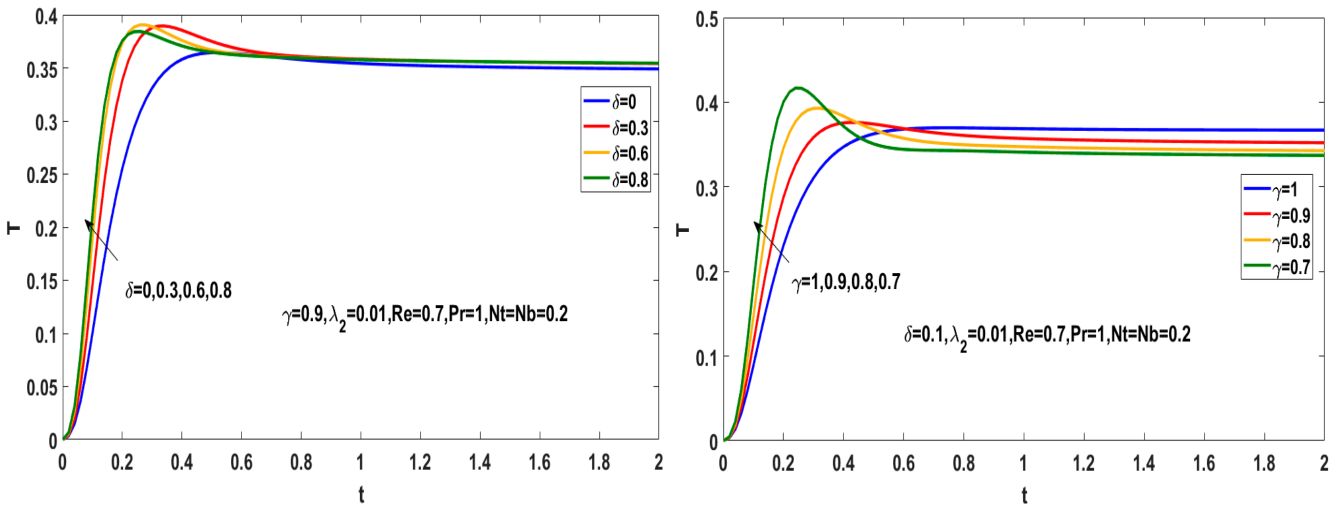

(**a**) (**b**)

Figure 4. Temperature distributions with respect to t: (**a**) for different δ; (**b**) for different γ.

5.2. Effects of the Fractional Parameters on the Concentration Field

Figure 5 describes the influence of different fractional parameters δ and γ on the concentration of nanofluids in the y direction. The result from Figure 5a shows that the concentration of nanofluids presents a downward trend with the enlargement of fractional parameter δ; that is, the distribution of nanoparticles becomes more sparse in the same region of y. This is mainly because the increase in the temperature reduces the concentration of nanoparticles in the flow region. When $\delta = 0.1$, the concentration distributions for different parameter γ are given in Figure 5b. As the fractional parameter γ decreases, the concentration presents a downward trend. Overall, the above results demonstrate that the fractional parameters δ and γ affect the movement of nanoparticles by changing the temperature, and then affect the mass transfer process of nanofluids.

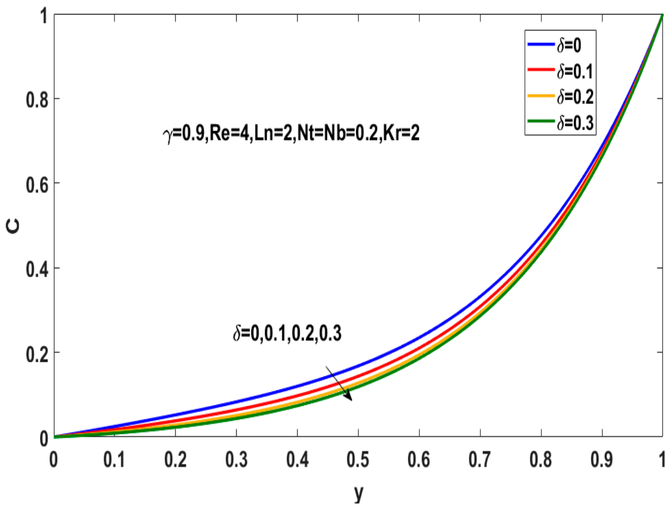

(**a**) (**b**)

Figure 5. Concentration distributions with respect to y: (**a**) for different δ; (**b**) for different γ.

The influence of different fractional order parameters δ and γ on concentration distribution in the t direction is shown in Figure 6. As can be seen in Figure 6a, with the rise in parameter δ, the peak value of concentration distribution decreases, but eventually tends to be stable. Figure 6b shows the concentration distributions under different fractional parameter γ. The peak of the concentration rises as the value of γ increases. It is because the increase in temperature difference of nanofluids leads to the enhancement of the thermophoresis of nanoparticles and the nanoparticles quickly shift from the higher temperature district to the lower temperature district, making the concentration of the nanoparticles decrease and reach the stable state more rapidly.

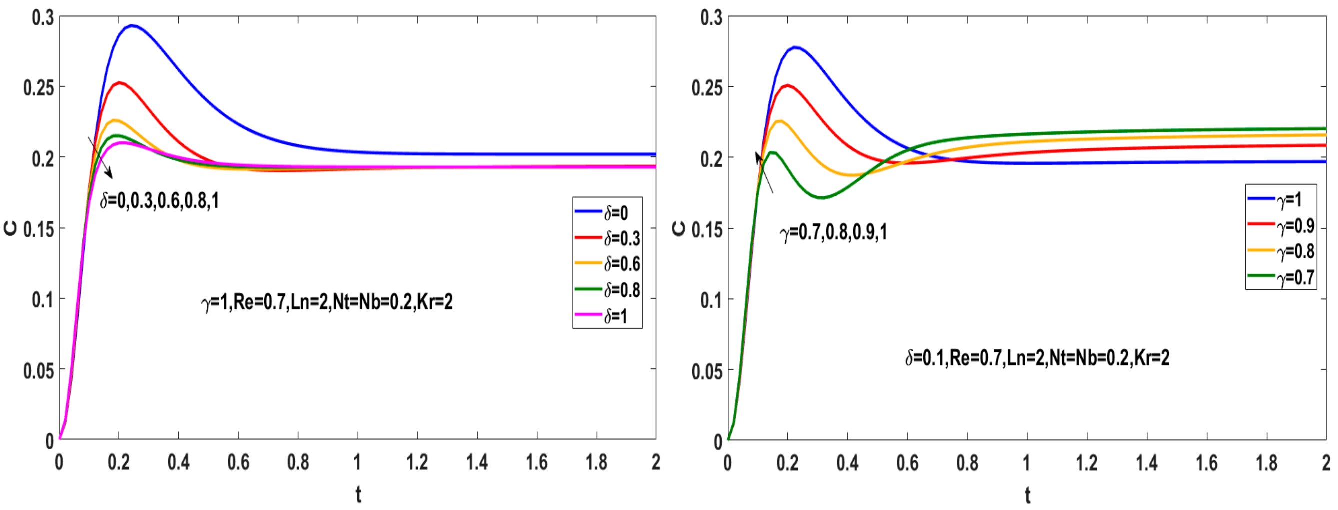

(**a**) (**b**)

Figure 6. Concentration distributions with respect to t: (**a**) for different δ; (**b**) for different γ.

5.3. Effects of Nb and Nt

Figure 7 describes the temperature and concentration distributions with different Brownian motion parameter Nb. Figure 7a displays that the temperature change rate increases with the rise in Nb. Physically, the adding of Brownian motion contributes to the efficient movement of nanoparticles between plates, thus, improving the heat transfer efficiency of nanofluids. Different from the temperature, the concentration gradually descends with larger Nb. The performances of different thermophoresis parameter Nt on temperature and concentration distributions are shown in Figure 8. The temperature presents an upward trend with the augment of Nt, which is due to the effect of heat capacity of nanoparticles. However, the improvement in the thermophoresis results in a decrease in concentration, which is consistent with the results [36]. Therefore, the enhancement of Brownian diffusion and thermophoresis promotes the heat transfer of nanofluids, which plays a crucial part in the diffusion process of nanoparticles.

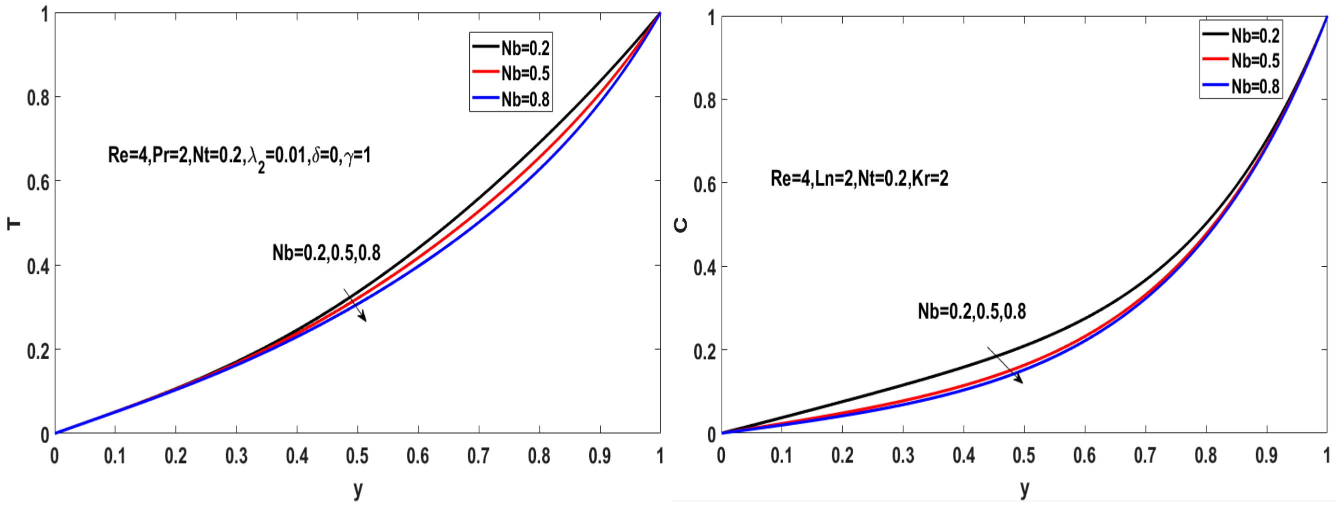

(**a**) (**b**)

Figure 7. Effects of Nb: (**a**) on temperature distributions; (**b**) on concentration distributions.

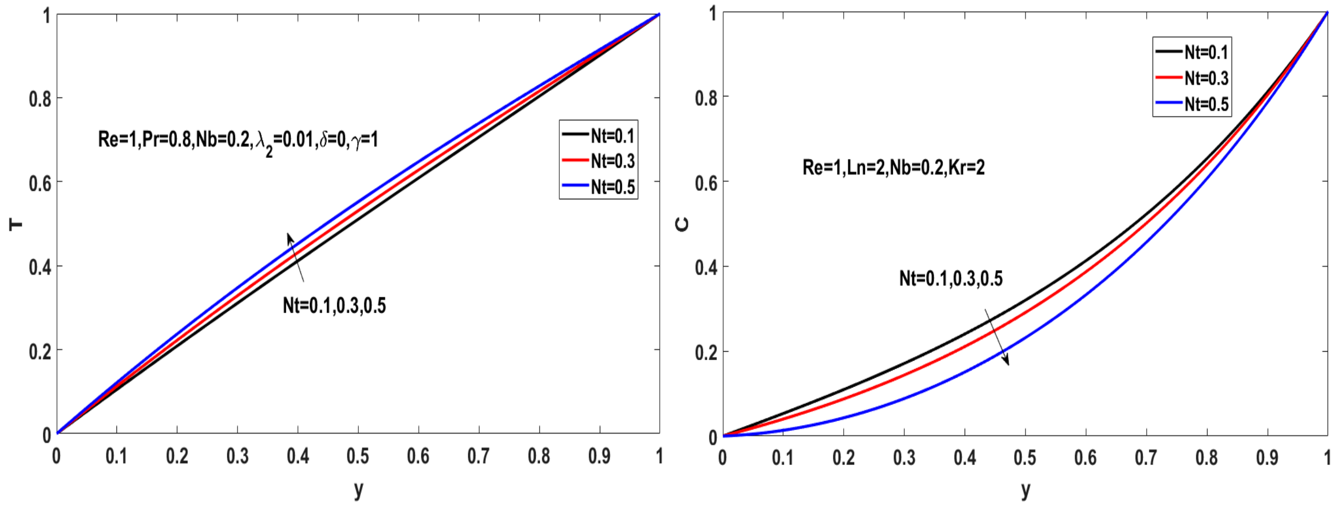

(**a**) (**b**)

Figure 8. Effects of Nt: (**a**) on temperature distributions; (**b**) on concentration distributions.

6. Conclusions

In this paper, we investigate the mixed convection of fractional nanofluids considering Brownian motion and thermophoresis. The arithmetic solutions of the fractional equations are obtained by employing the finite difference method. The effects of fractional order parameters, Brownian motion parameters, and thermophoresis parameters on the temperature and concentration are discussed. The consequences manifest that the rise in fractional parameter δ enhances the energy transfer process of nanofluids, while the augment of fractional parameter γ weakens the heat transfer. However, the opposite effects are found in the concentration distribution. In fact, the change in temperature affects the effective movement of nanoparticles, which is also an important reason for the increase and decrease in concentration. In addition, the enhancement of Brownian diffusion and thermophoresis promotes the heat transfer of nanofluids, which plays a crucial part in the diffusion process of nanoparticles.

Author Contributions: Y.T. and M.C.: formal analysis and computed the numerical results; Y.T. and X.C.: writing—review and editing; Y.T. and W.Y.: analyzed the results; M.C.: funding acquisition. All authors have read and agreed to the published version of the manuscript.

Funding: The work was supported by the National Natural Science Foundations of China under grant No. 51971031.

Data Availability Statement: Not applicable.

Acknowledgments: The authors would like to express their gratitude to the anonymous reviewers for their valuable comments on the improvement of this paper.

Conflicts of Interest: The authors declare no conflict of interest.

Nomenclature

$\boldsymbol{q}$	Heat flux
k	Thermal conductivity
K	Permeability
h_p	Specific enthalpy
T	Nanofluids temperature
$\boldsymbol{j}_p$	Diffusion mass flux
D_B	Brownian diffusion coefficient
D_T	Thermophoresis diffusion coefficient
E	Shear modulus
$\boldsymbol{p}$	Pressure
g	Gravitational acceleration
k_r	Chemical reaction parameter
Re	Reynolds number
Gr	Grashof number
Pr	Generalized Prandtl number
Nt	Thermophoresis parameter
Nb	Brownian motion parameter
Ln	Lewis number
Greek Symbols	
$\alpha, \beta, \delta, \gamma$	Time fractional derivative parameters
τ	Shear stress
ε	Shear strain
μ	Dynamic viscosity
λ_1	Relaxation time
λ_2	Temperature relaxation time
ρ_p	Mass density
ρ_{nf}	Density of the nanofluids
$(\rho\beta)_{nf}$	Thermal expansion coefficient
$(\rho c_p)_{nf}$	Capacitance
σ	Heat capacity of nanoparticle materials
υ	Kinematic viscosity
Γ	Gamma function
Subscripts	
nf	Nanofluids
p	Nanoparticles
ω	Wall condition
Superscript	
$*$	Dimensionless form

References

1. Fan, T.; Xu, H.; Pop, I. Mixed convection heat transfer in horizontal channel filled with nanofluids. *Appl. Math. Mech.* **2013**, *34*, 339–350. [CrossRef]
2. Abu-Nada, E.; Chamkha, A.J. Mixed convection flow of a nanofluid in a lid-driven cavity with a wavy wall. *Int. Commun. Heat Mass Transf.* **2014**, *57*, 36–47. [CrossRef]
3. Aaiza, G.; Khan, I.; Shafie, S. Energy transfer in mixed convection MHD flow of nanofluid containing different shapes of nanoparticles in a channel filled with saturated porous medium. *Nanoscale Res. Lett.* **2015**, *10*, 490. [CrossRef]

4. Aman, S.; Khan, I.; Ismail, Z.; Salleh, M.Z. Impacts of gold nanoparticles on MHD mixed convection Poiseuille flow of nanofluid passing through a porous medium in the presence of thermal radiation, thermal diffusion and chemical reaction. *Neural Comput. Appl.* **2018**, *30*, 789–797. [CrossRef] [PubMed]
5. Chakravarty, A.; Datta, P.; Ghosh, K.; Sen, S.; Mukhopadhyay, A. Mixed convective heat transfer in an enclosure containing a heat-generating porous bed under the influence of bottom injection. *Int. J. Heat Mass Transf.* **2018**, *117*, 645–657. [CrossRef]
6. Khanafer, K.; Vafai, K. Double-diffusive mixed convection in a lid-driven enclosure filled with a fluid-saturated porous medium. *Numer. Heat Transf.* **2002**, *42*, 465–486. [CrossRef]
7. Moolya, S.; Anbalgan, S. Optimization of the effect of Prandtl number, inclination angle, magnetic field, and Richardson number on double-diffusive mixed convection flow in a rectangular domain. *Int. Commun. Heat Mass Transf.* **2021**, *126*, 105358. [CrossRef]
8. Shankar, B.M.; Kumar, J.; Shivakumara, I.S. Magnetohydrodynamic instability of mixed convection in a differentially heated vertical channel. *Eur. Phys. J. Plus.* **2019**, *134*, 53. [CrossRef]
9. Shankar, B.M.; Kumar, J.; Shivakumara, I.S. Stability of mixed convection in a differentially heated vertical fluid layer with internal heat sources. *Fluid Dyn. Res.* **2019**, *51*, 055501. [CrossRef]
10. Mahian, O.; Bellos, E.; Markides, C.N.; Taylor, R.A.; Wongwises, S. Recent advances in using nanofluids in renewable energy systems and the environmental implications of their uptake. *Nano Energy* **2021**, *86*, 106069. [CrossRef]
11. Esfe, M.H.; Bahiraei, M.; Mir, A. Application of conventional and hybrid nanofluids in different machining processes: A critical review. *Adv. Colloid Interface Sci.* **2020**, *282*, 102199. [CrossRef]
12. Nikolov, A.; Wu, P.K.; Wasan, D. Structure and stability of nanofluid films wetting solids: An overview. *Adv. Colloid. Interface Sci.* **2019**, *264*, 1–10. [CrossRef] [PubMed]
13. Choi, S.U.S.; Eastman, J.A. Enhancing thermal conductivity of fluids with nanoparticles. *Asme. Fed.* **1995**, *231*, 99–105.
14. Xuan, Y.M.; Li, Q. Heat transfer enhancement of nanofluids. *Int. J. Heat Fluid Flow* **2000**, *21*, 58–64. [CrossRef]
15. Buongiorno, J. Convective transport in nanofluids. *J. Heat Transf.* **2006**, *128*, 240–250. [CrossRef]
16. Ahmed, S.E.; Rashed, Z.Z. MHD natural convection in a heat generating porous medium-filled wavy enclosures using Buongiorno's nanofluid model. *Case Stud. Therm. Eng.* **2019**, *14*, 100430. [CrossRef]
17. Bänsch, E.; Faghih-Naini, S.; Morin, P. Convective transport in nanofluids: The stationary problem. *J. Math. Anal. Appl.* **2020**, *489*, 124151. [CrossRef]
18. Sohail, N.; Wang, F.Z.; Fahad, M.A.; Farrah, S. Numerical computations for Buongiorno nano fluid model on the boundary layer flow of viscoelastic fluid towards a nonlinear stretching sheet. *Alex. Eng. J.* **2022**, *61*, 1769–1778.
19. Rana, P.; Gupta, G. Numerical and sensitivity computations of three-dimensional flow and heat transfer of nanoliquid over a wedge using modified Buongiorno model. *Comput. Math. Appl.* **2021**, *101*, 51–62. [CrossRef]
20. Puneeth, V.; Anandika, R.; Manjunatha, S. Implementation of modified Buongiorno's model for the investigation of chemically reacting $rGO - Fe_3O_4 - TiO_2 - H_2O$ ternary nanofluid jet flow in the presence of bio-active mixers. *Chem. Phys. Lett.* **2022**, *786*, 139194. [CrossRef]
21. Kulish, V.V.; Lage, J.L. Application of fractional calculus to fluid mechanics. *J. Fluids Eng.* **2002**, *124*, 803–806. [CrossRef]
22. Liu, F.; Turner, I.; Anh, V. An unstructured mesh finite volume method for modelling saltwater intrusion into coastal aquifers. *J. Comput. Appl. Math.* **2002**, *9*, 391–407. [CrossRef]
23. Aman, S.; Khan, I.; Ismail, Z.; Salleh, M.Z.; Tlili, I. A new caputo time fracional model for heat transfer enhancement of water based graphene nanofluid: An application to solar energy. *Results Phys.* **2018**, *9*, 1352–1362. [CrossRef]
24. Zhao, J.H.; Zheng, L.C.; Zhang, X.X.; Liu, F.W. Unsteady natural convection boundary layer heat transfer of fractional Maxwell viscoelastic fluid over a vertical plate. *Int. J. Heat Mass Transf.* **2016**, *97*, 760–766. [CrossRef]
25. Chen, X.H.; Ye, Y.F.; Zhang, X.R.; Zheng, L.C. Lie-group similarity solution and analysis for fractional viscoelastic MHD fluid over a stretching sheet. *Comput. Math. Appl.* **2018**, *75*, 3002–3011. [CrossRef]
26. Liu, L.; Zheng, L.C.; Liu, F.W.; Zhang, X.X. Heat conduction with fractional Cattaneo-Christov upper-convective derivative flux model. *Int. J. Therm. Sci.* **2017**, *112*, 421–426. [CrossRef]
27. Cao, Z.; Zhao, J.H.; Wang, Z.J.; Liu, F.W.; Zheng, L.C. MHD flow and heat transfer of fractional Maxwell viscoelastic nanofluid over a moving plate. *J. Mol. Liq.* **2016**, *222*, 1121–1127. [CrossRef]
28. Zhao, J.H.; Zheng, L.C.; Chen, X.H.; Zhang, X.X.; Liu, F.W. Unsteady marangoni convection heat transfer of fractional Maxwell fluid with Cattaneo heat flux. *Appl. Math. Model.* **2017**, *44*, 497–507. [CrossRef]
29. Chen, X.H.; Yang, W.D.; Zhang, X.R.; Liu, F.W. Unsteady boundary layer flow of viscoelastic MHD fluid with a double fractional Maxwell model. *Appl. Math. Lett.* **2019**, *95*, 143–149. [CrossRef]
30. Tan, W.C.; Pan, W.X.; Xu, M.Y. A note on unsteady flows of a viscoelastic fluid with the fractional Maxwell model between two parallel plates. *Int. J. Non-Linear Mech.* **2003**, *38*, 645–650.
31. Yang, W.D.; Chen, X.H.; Zhang, X.R.; Zheng, L.C.; Liu, F.W. Flow and heat transfer of double fractional Maxwell fluids over a stretching sheet with variable thickness. *Appl. Math. Model.* **2020**, *80*, 204–216. [CrossRef]
32. Yang, W.D.; Chen, X.H.; Jiang, Z.Y.; Zhang, X.R.; Zheng, L.C. Effect of slip boundary condition on flow and heat transfer of a double fractional Maxwell fluid. *Chin. J. Phys.* **2020**, *68*, 214–223. [CrossRef]
33. Shen, M.; Chen, L.L.; Zhang, M.C.; Liu, F.W. A renovated Buongiorno's model for unsteady sisko nanofluid with fractional Cattaneo heat flux. *Int. J. Heat Mass Transf.* **2018**, *126*, 277–286. [CrossRef]

34. Zhang, M.C.; Shen, M.; Liu, F.W.; Zhang, H.M. A new time and spatial fractional heat conduction model for Maxwell nanofluid in porous medium. *Comput. Math. Appl.* **2019**, *78*, 1621–1636. [CrossRef]
35. Shen, M.; Chen, S.R.; Liu, F.W. Unsteady MHD flow and heat transfer of fractional Maxwell viscoelastic nanofluid with Cattaneo heat flux and different particle shapes. *Chin. J. Phys.* **2018**, *56*, 1199–1211. [CrossRef]
36. Sayehvand, H.O.; Parsa, A.B. A new numerical method for investigation of thermophoresis and Brownian motion effects on MHD nanofluid flow and heat transfer between parallel plates partially filled with a porous medium. *Results Phys.* **2017**, *7*, 1595–1607. [CrossRef]